This paper is available online at www.praiseworthyprize.org
International Review of Mechanical Engineering (I.RE.M.E.), Vol. 12, N. 8
ISSN 1970 - 8734 August 2018

A Geometric Algorithm for Redundant Inverse Kinematics with Obstacle Avoidance in a Known Environment

Kun Wang[1,2,3], Wang Qi[1], Huapeng Wu[3], Kun Jiang[4]

Abstract – *This paper proposes a geometric method for solving the inverse kinematics (IK) of redundant manipulators while satisfying the collision avoidance criterion. The proposed approach focuses on creating an algorithm for solving the redundant inverse kinematics (RIK) of manipulators in a known environment. Central to the method is the creation of an explicit expression of C-free space of the manipulators by using two new notions, named "inverse Denavit–Hartenberg (D–H) variables" and "interval function". Thus, a single optimized solution far from the obstacles is obtained automatically by exploring in the C-free space, following the principle of selecting the median value of the interval function preferentially. The proposed method is demonstrated using a snake robot, the EAST Articulated Maintenance Arm (EAMA), which is utilized in the EAST (Experimental Advanced Superconducting Tokamak) for maintenance tasks in the vacuum vessel. C-free space of EAMA in EAST is created based on the Obstacle Topology Partition Projection (OTPP) approach and formulated by the interval functions. With the expression of C-free space, a single optimum solution is obtained during the exploration that starts at the end position or pose of the extremity point Pend. Eventually, several tip positions of EAMA are sampled to test the accuracy and correctness of the algorithm.*

Keywords: *Redundant Inverse Kinematics, Inverse DH Variables, C-Free Space, Interval Function, EAMA*

Nomenclature

C-space (Q)	Configuration space
C_{free}	C-free space
$C_{obstacle}$	C space obstacles
D–H	Denavit–Hartenberg convention
EAST	Experimental Advanced Superconducting Tokamak
EAMA	EAST Articulated Maintenance Arm
IFUN	Interval function
IK	Inverse kinematics
OTPP	Obstacle Topology Partition Projection
P_w	Position and oriented workspace
P_{end}	End position or pose of the extremity point
Q, Q_1, Q_2	Configuration of a n-dimensional manipulator
$q_1, q_2, \ldots, q_n$	Joint variables
$\theta_1, \theta_2, \ldots, \theta_n$	Inverse DH variables
$\widehat{P_{i-1}}$	Connection point between link i−1 and link i
RIK	Redundant inverse kinematics
RH	Remote handling
${}^{i-1}_{i}T$	4×4 homogeneous matrix from frame i−1 to frame i
α_i, a_i, d_i and q_i	DH parameters used in the modified DH convention

I. Introduction

In the last decade, remote handling (RH) technology has been developed for fusion reactor maintenance [1]-[2] and some devices have been constructed for its application, for example, ITER, JET and EAST.

However, as most vacuum vessels are narrow and deep, maintenance must be performed by manipulators that have redundant joints to provide the required dexterity. The extra DOFs can be used to avoid joint limits and to circumvent obstacles in the workspace, while still reaching a desired end-effector pose in the task space [3]-[17]. Consequently, the problem of redundant inverse kinematics (RIK) must be addressed in the control of the redundant manipulator.

The RIK and inverse kinematics of a non-redundant manipulator are equivalent, in the sense that they involve calculation of solutions of the joint variables under generic point P_{end} or the pose of the end-effector.

However, the extra DOFs make a manipulator kinematically different from a non-redundant system.

Specifically, the RIK has an infinite number of solutions, and evaluation criteria for system control are

Available online by August 31th, 2018 https://doi.org/10.15866/ireme.v12i8.13524

thus necessary to find the most suitable solution. The most important criteria in solutions of the RIK are joint limit avoidance, computational efficiency and optimization of solutions, especially obstacle avoidance.

Many algorithms have been proposed to meet the task requirements and solution criteria, for example the pseudo inverse-based Jacobian method, genetic algorithms [5]-[16], neural networks [4], algebraic methods [6] and geometric methods [7]. The most general algorithm for solving RIK are Jacobian pseudo inverse-based techniques, and these are widely used to deal with the redundancy resolution problem [8].

However, the Jacobian method has some drawbacks such as a lack of repeatability, low computational efficiency, and poor convergence when dealing with coupling manipulators. Hence, some other algorithms are proposed for improving the efficiency. The authors in [9] proposed an approach to solve the redundancy resolution problem in a known environment using forward kinematics functions and neural network in the inverse modelling manner, which also meets the requirement of obstacle avoidance. It is generally accepted that geometric methods are capable of finding a closed-form single optimum solution depending upon the path in the environment and are efficient at solving the RIK with some criteria. L. Sardanna et al. [10] presented a geometric approach for solving the RIK of a 4-link robot for surgical tasks. The RIK are solved through a graphic method, i.e., calculating intersection points between circles of each link. Srinivas Neppalli et al. [11] treated a redundant manipulator as a multi-section continuum robot, and the RIK were solved based on a single continuum section trunk. In fusion field, a geometric approach for solving the RIK of a flexible manipulator-EAST Articulated Maintenance Arm (EAMA) has been demonstrated in [12]. The authors presented an approach named as “OTPP” for creating a collision-free space of EAMA, and searching further in the space to get a solved configuration far away from the environment.

This paper focuses on formalizing and extending the approach in [12] to solve RIK while satisfying the collision avoidance criterion. The novelty of this paper lies in the division of the collision-free space depending on the links of a robot and explicitly calculating the interval of each link, which is a function of the geometric features of the link and the known environment. Consequently, the RIK problem is equivalent to a depth-first search problem. The searched solution is not only collision-free but also guarantees safety, i.e., it stays far from the obstacles. In particular, it is very efficient to solve the RIK problem with surrounding organs, as compared to other RIK algorithms.

II. Methods

The proposed algorithm in [12] attempts to eliminate redundancies through hybrid use of geometry and the searching method.

In addition, owing to the continuity mapping from joint space to Euclidean space, the exploring process adopts the principle of selecting the median configuration preferentially. Therefore, the computation of the method is based on the calculation of C-free space, after which an optimal solution can be obtained by searching in the solved C-free space.

II.1. C-Free Space

The configuration space (C-space) is the space of the configurations of the manipulator [13]. C-space consists of any set of generalized coordinates, and it can be decomposed into C-space obstacles and C-free space. C-space obstacles represent the mapping of obstacles from Euclidean space to C-space. C-free space is defined as the complement of the C-space obstacles.

Mathematically, let:

$$Q = Q_1(q_1, q_2, ..., q_n) = Q_2(P_{end}, \theta_n, \theta_{n-1}, ..., \theta_1) \quad (1)$$

denoting the configuration of an n-dimensional manipulator with n rigid links and n joints, where P_{end} denotes the pose and position of the end-effector of the manipulator. q_i is the generalized variable of the i-th joint used in the modified Denavit–Hartenberg (D–H) convention, q_1 and q_n are the joint variables of the first and the last joint, respectively. Another set of joint variables θ combined with P_{end}, which are named as "inverse DH variables", are introduced to describe the kinematics structure of the manipulator in another manner. The variable θ_i is defined as the revolute angle around axis Z_i from X_i to X_{i-1} according to the right-hand rule or displacement of two original points from frame i to frame $i-1$. The definition of the two joint variables is illustrated in Fig. 1(a), where $\widehat{P_{i-1}}$ is the connection point between link $i-1$ and link i. Clearly, θ_i is equal to $-q_i$ as shown in Fig. 1(b). Thus, the expressions of the transformation matrices of the manipulator are:

$${}^{i-1}_{i}T = rot(X, \alpha_i)trans(X, a_i)rot(Z, q_i)trans(Z, d_i) \quad (2)$$

$$\begin{aligned} {}^{i}_{i-1}IT &= ({}^{i-1}_{i}T)^{-1} = (trans(Z, d_i))^{-1}(rot(Z, q_i))^{-1} \\ &(trans(X, a_i))^{-1}(rot(X, \alpha_i))^{-1} = \\ &= (trans(Z, d_i))^{-1} rot(Z, \theta_i) \\ &(trans(X, a_i))^{-1}(rot(X, \alpha_i))^{-1} \end{aligned} \quad (3)$$

where α_i, a_i, d_i and q_i are the DH parameters used in the modified DH convention. ${}^{i-1}_{i}T$ is the 4×4 homogeneous matrix from frame i−1 to frame I, and ${}^{i}_{i-1}IT$ is the inverse 4×4 homogeneous matrix from frame i to frame i−1. Moreover, the two matrices are functions of joint variables q_i and θ_i, respectively. Recursively, the kinematics equations are:

$$T = P_{end} = {}^{0}_{1}T \dots {}^{n-1}_{n}T \, {}^{end}_{n}T \tag{4}$$

$$I = P_{end} \, ({}^{end}_{n}T)^{-1} \, {}^{n}_{n-1}IT \dots {}^{2}_{1}IT * ({}^{1}_{0}T)^{-1} \tag{5}$$

where T is the position and pose of end effector in the base frame; I is the identity matrix; and ${}^{end}_{n}T$ represents a constant transformation matrix from the frame n to the end effector as shown in Fig. 1(b). Eq. (4) and Eq. (5) reveal that kinematics structures of the manipulator can be formulated by two kinds of joint variables: DH variables and inverse DH variables.

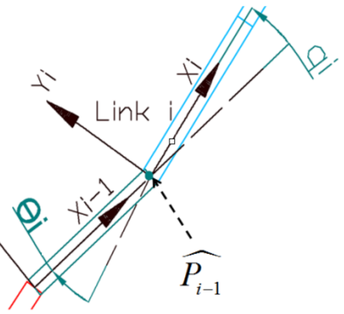

(a)

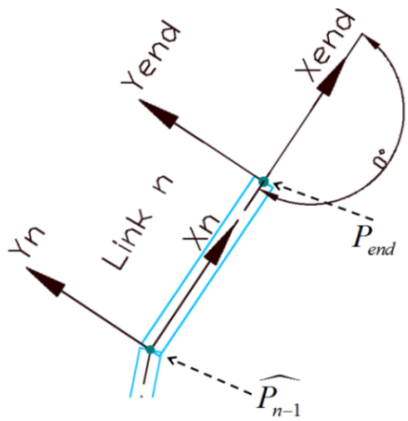

(b)

Figs. 1 (a). Description of inverse DH variables (b). Inverse DH variables of the last link

In this paper, DH variables are used instead of DH variables for describing C space and C-free space:

$$C = \{Q_2(P_{end}, \theta_i) \,|\, (P_{end} \in P_w, \theta_i \in [-\beta_i, -\alpha_i])\} \tag{6}$$

where α_i and β_i are the lower and upper limits belonging to joint-i, respectively. P_w represents the position and oriented workspace of the manipulator, and C is the C-space. Then, the other spaces can be written as:

$$\begin{gathered} C_{free} = \{Q_2(P_{end}, \theta_i) \,|\, P_{end} \in P_{free}, \\ \theta_i \in f_i(\widehat{P_{i-1}}, obstacle)\} \end{gathered} \tag{7}$$

$$C_{obstacle} = C - C_{free} \tag{8}$$

where P_{free} denotes a set of position and pose of end effectors in which an end effector can reach without collision; C_{free} and $C_{obstacle}$ are C-free space and C space obstacles, respectively.

The function $f_i(\hat{P}_{i-1}, obstacle), i = 1, 2, \dots, n$ in Eq. (7), which is named as "interval function (IFUN)", is introduced to represent legal ranges (position range of a joint without collision) of joint-i. For the i-th revolute joint, IFUN is a set of joint variables (inverse DH variables) under all the collision-free states of link i−1, when the connection point between link i−1 and link i is fixed at point $\widehat{P_{i-1}}$.

The parameter *obstacle* in IFUN denotes geometrical information of obstacles in the specific environment.

Point $\widehat{P_{i-1}}$ can be computed by Eq. (5) and inverse DH variables from θ_{i+1} to θ_n. Thus, IFUN can be written in the form:

$$f_i(\hat{P}_{i-1}, obstacle) = \bigcup_{j=1}^{m_i} ([\theta_i^j, \theta_i^{j+1}]) \cap [-\beta_i, -\alpha_i] \tag{9}$$

The interval $[\theta_i^j, \theta_i^{j+1}]$ is the j-th subset that belongs to the IFUN of joint i, and m_i is the number of the subset.

From Eq. (7) and Eq. (9), it can be observed that the key step of computation of C-free space is the determination of all the subsets.

II.2. Procedure of Solving RIK with IFUN

The RIK with the obstacle avoidance criterion are solved through exploration in C-free space, which is executed by a procedure described below:

1. The position and pose of end effector is inputted, and the coordinates of $\widehat{P_{n-1}}$ in the base frame are further calculated through the matrix ${}^{end}_{n}T$ in Eq. (5).
2. The obstacles are modelled based on their geometric characteristic, and all the subsets when the link n−1 is fixed at the point $\widehat{P_{n-1}}$ are calculated. IFUN $f_{n-1}(\widehat{P_{n-1}})$ can then be obtained through Eq. (9).
3. In order to keep far away from collision state, the principle that selecting the median value of IFUN preferentially is adopted to select an initial value of the last joint. The value is substituted into Eq. (3) to calculate point $\widehat{P_{n-2}}$ and further to compute $f_{n-2}(\widehat{P_{n-2}})$ using the same method as in step 2.
4. A value from the interval $f_{n-2}(\widehat{P_{n-2}})$ is similarly selected to calculate $\widehat{f_{n-3}}(\widehat{P_{n-3}})$ until the point $\hat{P}_1$ is obtained. Eventually, n−2 values are selected by recursive calculation.
5. The n−2 values are substituted into Eq. (5), and then it will be transformed into equations of the DH variables θ_1 and θ_2. If the solution exists and the first

link does not collide with any obstacles, the RIK problem is solved; otherwise, another n−2 value is chosen based on the same principle as step-3, and the procedure is repeated until a solution is found or the maximum cycle number is met, at which point the iteration ends. From the geometric viewpoint, the goal of step-5 is to check the existence of the intersection between the base and the first link. If the first joint of the manipulator is a revolute joint, the task of the step is to check if the point $\widehat{P}_1$ is on the circle whose centre locates at the point $\widehat{P}_0$, and the radius is the length of the first link. If the joint is a translational one, the circle is regressed into a line, as shown in Fig. 2.

6. If a solution is found, the n values are converted into DH variables. If not, failure is reported.

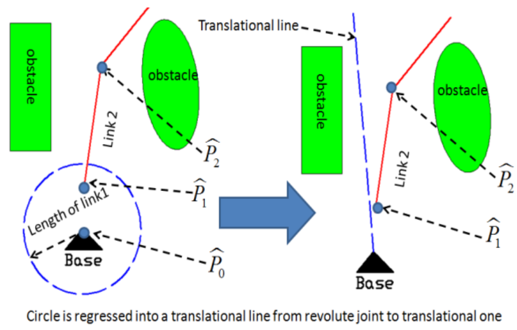

Fig. 2. Checking for the existence of the intersection of revolute and translational joints

II.3. A Simple Example

A simple redundant planar robot with four DOFs is presented to illustrate procedural considerations. The joint limit of the robot is defined as [−90°, 90°], and $C = \left\{ Q_2 \mid P_{end} \in P_w, \theta_i \in \left[-90^o, 90^o \right] \right\}$. The initial state of the robot is shown in Fig. 3(a), where the objects in green are the obstacles and the object in red is the planar robot. First, steps 1 and 2 are followed, as depicted in Figs. 3(b) and (c). The IFUN of joint 4 is:

$$f_4(\widehat{P}_4) = [\theta_4^1, \theta_4^2] \cap [-90^o, 90^o] = [15^o, 76^o]$$

Assuming the interval [15°, 76°] is divided into 20 segments, based on the median value principle, the selected value of θ_4 is:

$$t_4^{\,j} = \left(15^o + 76^o\right)/2 + \left(76^o - 15^o\right) \times k / 20 \quad (10)$$

$$k = \begin{cases} -j/2, (-1)^j > 0 \\ (j-1)/2, (-1)^j < 0 \end{cases} \quad (11)$$

where t_4^j is the selected value of θ_4 at the j-th cycle.

Second, during the first cycle, the value of θ_4 is chosen as 45.5°. Similarly, the IFUN of the third joint is evaluated such that:

$$f_3(\widehat{P}_3) = [\theta_3^1, \theta_3^2] \cap [-90^o, 90^o] = [-17^o, 90^o]$$

Figs. 3(d) and (e) depict the critical collision state of link-3 under $\theta_4 = t_4^1 = 45.5^o$. Selection of θ_3 will also follow the median value principle. During the j-th cycle, t_3^j is selected as the value of θ_3, and then θ_1 and θ_2 can be calculated immediately following step-5 in section 2.2. If no solution exists or there is a collision of the first link, the value of θ_3 is changed to t_3^{j+1} until a solution is found or the max cycle time is reached. Eventually, a solved configuration of the robot is found during the fifth cycle of joint-3 and the first cycle of joint-4, as shown in Fig. 3 (f). The solved configuration is given by:

$$Q = \begin{bmatrix} q_1 = -35.6^o, q_2 = 78.4^o, \\ q_3 = -\theta_3 = -47.2^o, q_4 = -\theta_4 = -45.5^o \end{bmatrix}$$

III. Solving RIK of EAMA

Similarly, RIK of EAMA in EAST vacuum vessel (VV) will also follow the procedure, which is the subject of section III. The focus here is to solve the problem of RIK (given the position of P_{n-1}) with collision avoidance for the 8-DOFs redundant manipulator EAMA in EAST VV through the procedure in section II.2.

III.1. Structure of EAMA

EAMA, 8-DOFs light-weight flexible arm, adopts a modular design. It is composed of five modules (7 rotation DOFs) and a displacement shutter (1 DOF).

Each module is equipped with a yaw joint that provides rotational motion, except the last two modules, which have both pitch and yaw joints, and these modules are linked with a parallelogram structure that keeps the yaw joint axis always vertical and the clevis horizontal.

This implies that auxiliary pitch joints Z_{4d} and Z_{6d} always have the opposite rotation angles relative to pitch joints Z_4 and Z_6, respectively [12]. Fig. 5 presents the cross-section of EAMA in EAST VV.

III.2. Calculation of IFUN of EAMA

Considering the geometric characteristics of the EAST VV, an approach called Obstacle Topology Partition Projection (OTPP) was presented in [12] to calculate legal motion ranges of a link in the EAST VV. The OTPP divides the calculation into two situations: link in the cylinder area and link in the conic area. In this study, we calculate IFUN based on OTPP.

In order to simplify the calculation, each module of EAMA is wrapped with oriented block boxes (OBBs), in order to provide a hierarchical way of deciding if two objects intersect [14].

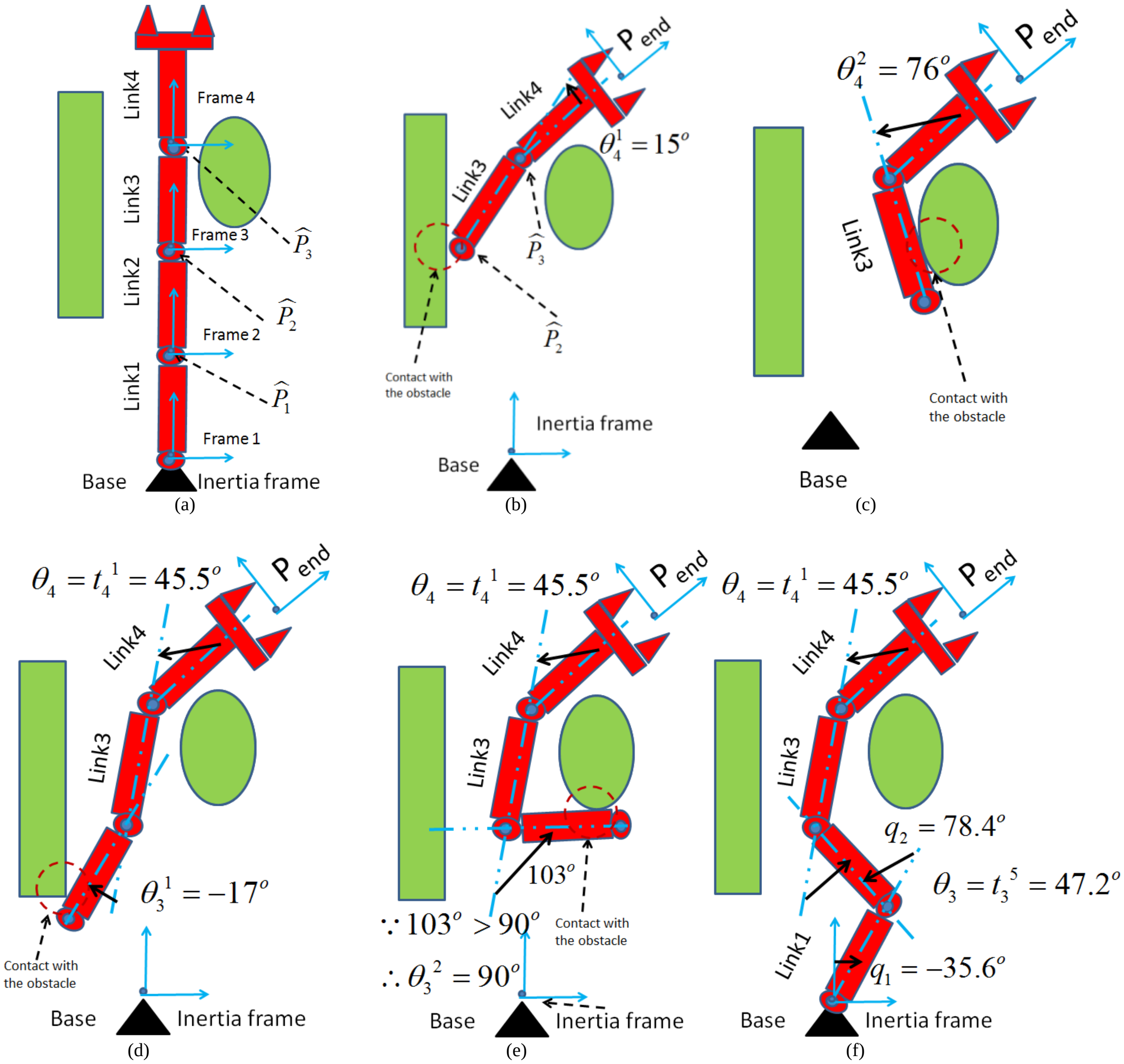

Figs. 3. (a) initial state of the planar robot (b) critical collision state_1 of link_3 (c) critical collision state_2 of link_3 (d) critical collision state_1 of link_2 (e) critical collision state_2 of link_2 (f) solved configuration of the planar robot

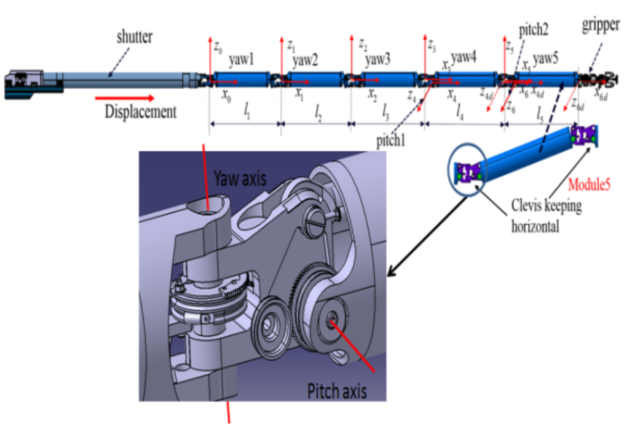

Fig. 4. Model and structure of EAMA

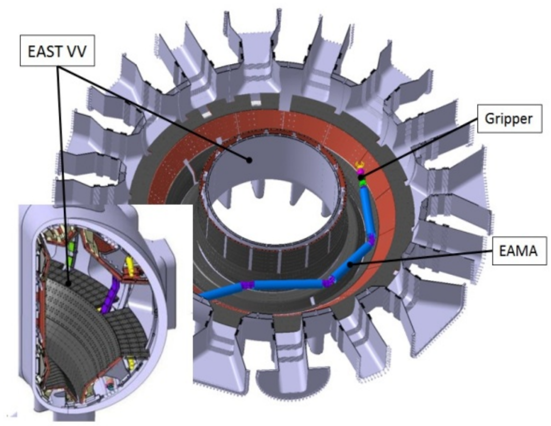

Fig. 5. Cross-section of EAMA together with EAST

Specifically, collision detection between objects is simplified to the distance between the boxes. As illustrated in Fig. 6, one module of EAMA consists of three OBBs.

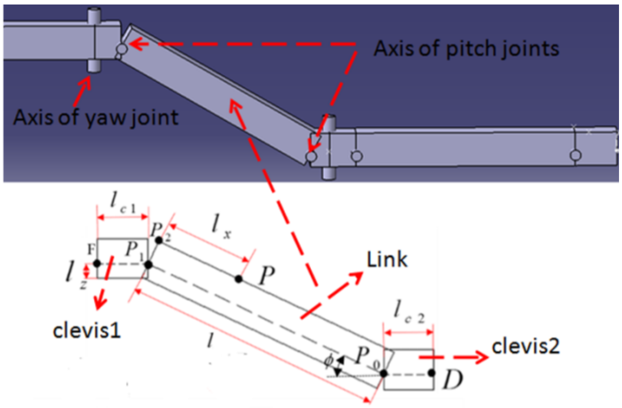

Fig. 6. OBBs of a module of EAMA

Finally, the flowchart of the calculation is illustrated in Fig. 7.

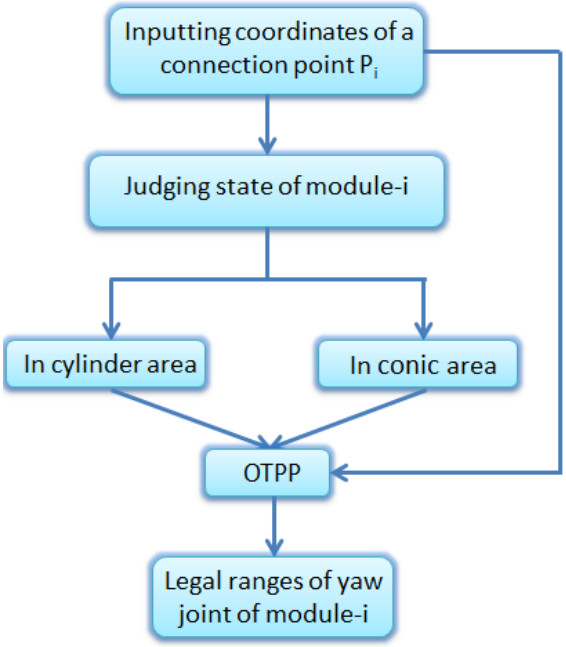

Fig. 7. Flowchart of calculation of IFUN

III.3. Solving EAMA's Configuration

After the IFUNs of every module of EAMA are obtained, steps 1 to 4 of the procedure described in section-2.2 can be completed. The fifth step is to solve the equations of the DH variables θ_1 and θ_2. From a geometric view, it is checked if the point $\widehat{P_1}$ of the first module (as shown in Fig. 2) is on the translational line, which is named the "shuttle line". The procedure for solving EAMA's RIK is summarized in Fig. 8.

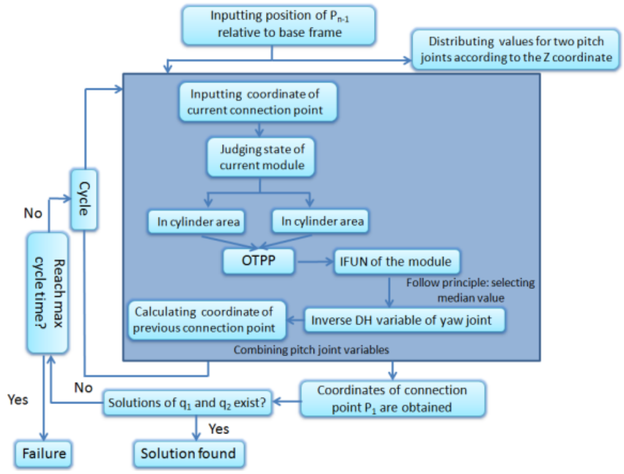

Fig. 8. Procedure for solving RIK of EAMA

IV. Simulation

In order to test the accuracy and correctness of the proposed algorithm for solving RIK of EAMA, six hundred target points, treated as input of the algorithm and shown in Fig. 9, are uniform random sampled in EAST VV from the entrance to the farthest location, and the methods for testing the two items are listed below.

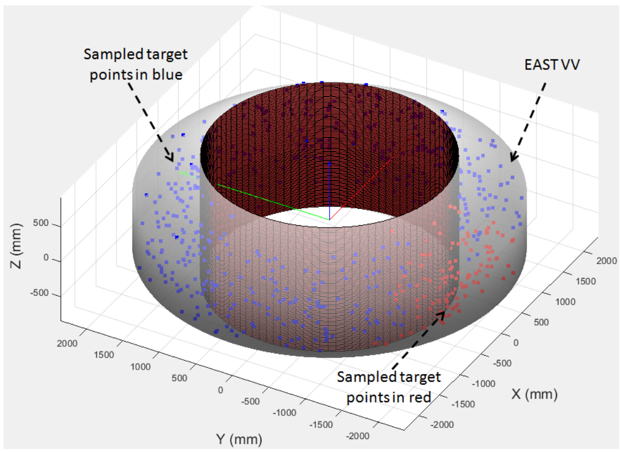

Fig. 9. Six hundred sampled target points in EAST VV (Only points in blue represent tip positions that EAMA can reach without collision)

First, the accuracy is determined. A solved configuration is substituted into Eq. (4) to get the position of the end effector and further calculate the deviation between the position and input of the algorithm. Therefore, the accuracy can be evaluated as:

$$Accuracy = 1 - norm\left(\left(P_1 - P_2\right)\right) / norm\left(P_1\right) \quad (12)$$

where P_1 is input of the algorithm and P_2 is the position calculated through Eq. (4); "norm" represents the norm operation of a vector. Second, the correctness is calculated by checking the collision state and calculating minimal distance between EAMA and its circumstance for a solved configuration through an open software called RobWork [15]. Fig. 11 illustrates the results of the accuracy among the sampled target points with which collision-free configurations can be calculated and obtained.

Fig. 12 shows the minimal distances between EAST VV and EAMA under the solved configurations. Coordinates of these points can be observed in Fig. 9 and Fig. 10. Points in blue represent sampled target points with a solution, and points in red denote positions that EAMA cannot reach without collision.

Based on the results of simulation, accuracy and collision avoidance are demonstrated.

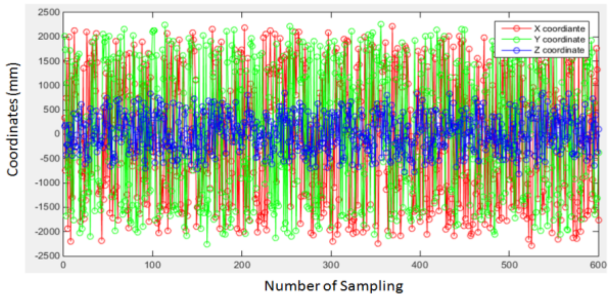

Fig. 10. Coordinates of these sampled target points

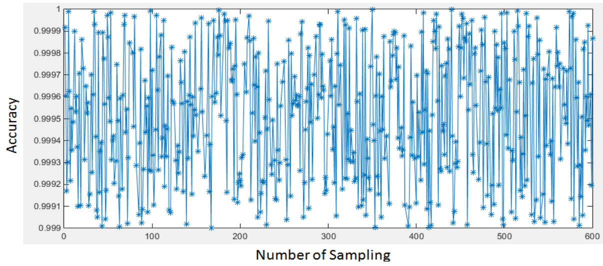

Fig. 11. Accuracy of sampled target points with a solution exists

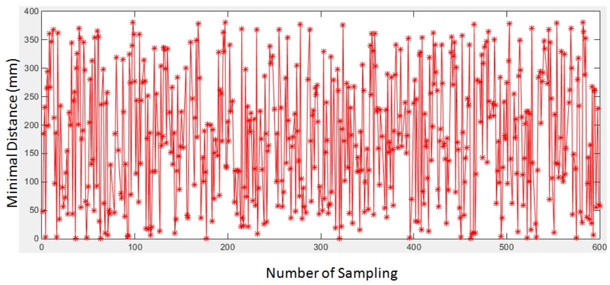

Fig. 12. Minimal distance of sampled target points with solution exists

V. Discussion and Conclusion

A geometry-based algorithm for solving RIK of manipulators with satisfaction of collision avoidance is proposed and simulated. The key calculation of the method is C-free space and IFUN. Taking an n-DOFs manipulator for example, given a desired tip position or pose, the algorithm first focuses on creating IFUNs of each link and further explores among the n IFUNs based on the principle of selecting median values preferentially to get a solved configuration, which is far from the environment. This method is efficient for solving RIK and avoiding collisions in a known environment, especially a tokamak-like environment.

Acknowledgements

This work is supported by the China National Special Project for Magnetic Confinement Fusion Science Program through Grant No. 2014GB101003. The authors would like to express their sincere gratitude to all the members of the team.

References

[1] L. Gargiulo, P. Bayetti, V. Bruno, ITER Articulated Inspection Arm (AIA): Geometric calibration issues of a long-reach flexible robot, *Fusion Engineering and Design*, 83 (2008)1833–1836.

[2] H. P. Wu, H. Handroos, P. Pessi, J. Kilkki, L. Jones, Heikki Handroos, Pekka Pessi, Juha Kilkki, Lawrence Jones, Development and control towards a parallel water hydraulic weld/cut robot for machining processes in ITER vacuum vessel *Fusion Engineering and Design* 75–79 (2005) 625–631.

[3] Fahimi, Farbod, Autonomous Robots: *Modeling, Path Planning, and Control*, Springer (2009). 15-16.

[4] Hamid Toshani Opens, et al., Real-time inverse kinematics of redundant manipulators using neural networks and quadratic programming: A Lyapunov-based approach, *Robot. Auton. Syst.* 62 (6) (2014) 766–781.

[5] A. R. Khoogar, J. K. Parker, Obstacle avoidance of redundant manipulators using genetic algorithms, in: *IEEE Proceedings of Southeastcon '91*, 07–10 April 1991, Williamsburg, 1(1991) 317–320.

[6] A. Perez, J. M. McCarthy, Clifford algebra exponentials and planar linkage synthesis equations, *Journal of Mechanical Design* 127 (2005) 931–940.

[7] S. Yahya, M. Moghavvemi, H. A. F. Mohamed, Geometrical approach of planar hyper-redundant manipulators: inverse kinematics, path planning and workspace, *Simulation Modelling Practice and Theory* 19(1) (2011) 406–422.

[8] V. Perdereau, C. Passi, M. Drouin, Real-time control of redundant robotic manipulators for mobile obstacle avoidance, *Robot. Auton. Syst.* 41 (1) (2002) 41–59.

[9] Z. Mao, T. C Hsia, Obstacle avoidance inverse kinematics solution of redundant robots by neural networks, *Robotica* 15 (1) (1997) 3-10.

[10] L. Sardana, et.al, A geometric approach for inverse kinematics of a 4-link redundant In-Vivo robot for biopsy. *Robot. Auton. Syst.* 61 2013 1306-1313.

[11] Srinivas Neppalli, et al., A Geometrical Approach to Inverse Kinematics for Continuum Manipulators. *2008 IEEE International Conference on Intelligent Robots and Systems*. 3565-3570.

[12] Kun Wang, et al., Inverse kinematics research using obstacle avoidance geometry method for EAST Articulated Maintenance Arm (EAMA), *Fusion Engineering and Design* (2017) 1-11.

[13] T. Lozano-Perez, A simple motion planning algorithm for general robot manipulators, *Perception and Robotics* (1986) 626-630.

[14] Stefan Gottschalk, Ming Lin, and Dinesh Manocha, OBBTree: A Hierarchical Structure for Rapid Interference Detection, In *Proceedings of ACM Siggraph*, pp. 171-180, 1996.

[15] L. P. Ellekilde, J. A. Jorgensen, Robwork: A flexible toolbox for robotics research and education[C]//Robotics (ISR), *2010 41st International Symposium on and 2010 6th German Conference on Robotics (ROBOTIK)*. VDE, (2010) 1-7.

[16] Mansour, G., Sagris, D., Tsagaris, A., CMM Path Planning, Position and Orientation Optimization Using a Hybrid Algorithm, (2017) *International Review of Mechanical Engineering (IREME)*, 11 (2), pp. 144-150.
doi: https://doi.org/10.15866/ireme.v11i2.10159

[17] Niola, V., Rossi, C., Savino, S., A New Mechanical Hand:

Theoretical Studies and First Prototyping, (2014) *International Review of Mechanical Engineering (IREME)*, 8 (5), pp. 835-844. doi: https://doi.org/10.15866/ireme.v8i5.1755.

Authors' information

[1]Institute of Plasma Physics, Chinese Academy of Sciences, Hefei, China.

[2]University of Science and Technology of China, Hefei, China.

[3]Lappeenranta University of Technology, Lappeenranta, Finland.

[4]Army Artillery and Air-defense Academy.

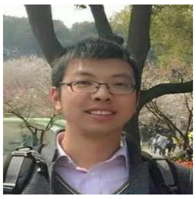

Kun Wang was born in 1988 in China, at a place called Anhui. Kun Wang is now a PhD student at the University of Science and Technology of China as well as at Lappeenranta University of Technology. His major field of study is kinematics algorithms in robotics. He has published a paper titled 'Inverse kinematics research using obstacle avoidance geometry method for EAST Articulated Maintenance Arm (EAMA)' in the journal Fusion Engineering and Design. His areas of interest are dynamics and kinematics control algorithms in robotics and their software design.

Qi Wang was born in 1990 in China, Anhui province. Qi Wang received a Master's degree at UTT in France in 2015. She currently works at the Institute of Plasma Physics, Chinese Academy of Sciences.
She has published a paper titled 'Design of a new light mechanical arm teaching software architecture'. Her major field of study is multi-body dynamics and motion control.

Huapeng Wu was born on 05.05.1964 in China, at a place called Wuhan. Huapeng Wu received a Bachelor's degree from the School of Mechanical Engineering, Huazhong University of Science and Technology (HUST) in 1986 and a Master's degree from the same school in 1990. In 2001, he received a Dr. Sc (Tech.) degree from the laboratory of Mechatronics, Lappeenranta University of Technology (LUT), Finland. His publications include 1) five books of which he is the associate chief editor and author; and 2) more than thirty journal articles and sixty international conference articles, two of which won the annual second-best paper prize. He has supervised 4 PhD theses, two postdoctoral students and several master's students. His research topics include brain control robots, robot design, inverse dynamic modelling and control of robots. He is also a reviewer with six SCI international journals.